RESEARCH ARTICLE

ANXIETY AND DEPRESSION ASSOCIATION OF AMERICA WILEY

Psychoradiological abnormalities in treatment-naive noncomorbid patients with posttraumatic stress disorder

Xueling Suo[1] | Du Lei[1,2] | Wenbin Li[1] | Huaiqiang Sun[1] | Kun Qin[1] |
Jing Yang[1] | Lingjiang Li[3] | Graham J. Kemp[4] | Qiyong Gong[1,5,6]

[1]Huaxi MR Research Center (HMRRC), Department of Radiology, West China Hospital of Sichuan University, Chengdu, Sichuan, China

[2]Department of Psychiatry and Behavioral Neuroscience, University of Cincinnati, Cincinnati, Ohio, United States

[3]Mental Health Institute, The Second Xiangya Hospital of Central South University, Changsha, Hunan, China

[4]Liverpool Magnetic Resonance Imaging Centre (LiMRIC) and Institute of Life Course and Medical Sciences, University of Liverpool, Liverpool, UK

[5]Research Unit of Psychoradiology, Chinese Academy of Medical Sciences, Chengdu, Sichuan, China

[6]Functional and Molecular Imaging Key Laboratory of Sichuan Province, Huaxi Xiamen Hospital of Sichuan University, Xiamen, Fujian, China

Correspondence
Qiyong Gong, Huaxi MR Research Center (HMRRC), Department of Radiology, West China Hospital of Sichuan University, No. 37 Guo Xue Xiang, Chengdu 610041, China.
Email: qiyonggong@hmrrc.org.cn

Abstract

Background: Neuroimaging studies in posttraumatic stress disorder (PTSD) have identified various alterations in white matter (WM) microstructural organization. However, it remains unclear whether these are localized to specific regions of fiber tracts, and what diagnostic value they might have. This study set out to explore the spatial profile of WM abnormalities along defined fiber tracts in PTSD.

Methods: Diffusion tensor images were obtained from 77 treatment-naive non-comorbid patients with PTSD and 76 demographically matched trauma-exposed non-PTSD (TENP) controls. Using automated fiber quantification, tract profiles of fractional anisotropy, axial diffusivity, mean diffusivity, and radial diffusivity were calculated to evaluate WM microstructural organization. Results were analyzed by pointwise comparisons, by correlation with symptom severity, and for diagnosis-by-sex interactions. Support vector machine analyses assessed the ability of tract profiles to discriminate PTSD from TENP.

Results: Compared to TENP, PTSD showed lower fractional anisotropy accompanied by higher radial diffusivity and mean diffusivity in the left uncinate fasciculus, and lower fractional anisotropy accompanied by higher radial diffusivity in the right anterior thalamic radiation. Tract profile alterations were correlated with symptom severity, suggesting a pathophysiological relevance. There were no significant differences in diagnosis-by-sex interaction. Tract profiles allowed individual classification of PTSD versus TENP with significant accuracy, of potential diagnostic utility.

Conclusions: These findings add to the knowledge of the neuropathological basis of PTSD. WM alterations based on a tract-profile quantification approach are a potential biomarker for PTSD.

KEYWORDS
automated fiber quantification, diffusion tensor imaging, posttraumatic stress disorder, psychoradiology, white matter

1 | INTRODUCTION

Posttraumatic stress disorder (PTSD) is a debilitating condition characterized by avoidance, re-experiencing, hyperarousal, and negative cognitions and mood (American Psychiatric Association, 2013), with major financial and public health impact (Kessler, 2000). Pathophysiological models of PTSD have widened focus from fronto–limbic circuitry to large-scale distributed networks (Ross and Cisler, 2020) whose key components are white matter (WM) tracts interconnecting gray matter regions (Ju et al., 2020). Diffusion tensor imaging (DTI) measurements of WM microstructural organization in vivo can help illuminate the pathophysiology of PTSD, and have potential as diagnosis/monitoring biomarkers.

DTI studies in PTSD report changes in fractional anisotropy (FA), a metric reflecting WM microstructural organization, in areas such as corpus callosum, cingulum, and superior longitudinal fasciculus (Daniels et al., 2013; Ju et al., 2020; Siehl et al., 2018). However, the reported location and nature of WM deficits varies: a recent review noted reports of both decreased and increased FA in cingulum across anterior, posterior, and dorsal subregions (Siehl et al., 2018). Why this variability? Most studies recruit relatively small samples, often heterogeneous, for example, including patients on medication or with psychiatric comorbidity, or including males and females without investigating sex-by-PTSD interaction. Furthermore, analyzing diffusion metrics along a tract provides information that may be missed by simple averaging (Yeatman et al., 2012); in trauma-exposed non-PTSD (TENP) subjects this approach revealed decreased FA in the left superior longitudinal fasciculus and increased FA in the left corticospinal tract (Meng et al., 2020). Finally, comparing TENP with non-traumatized healthy subjects makes it difficult to identify the effects of PTSD per se. The nature of WM alterations along fiber tracts over the early illness course in treatment-naïve (neither psychotherapy nor pharmacotherapy) PTSD patients without psychiatric comorbidity remain to be investigated.

We used a tract-profile quantification approach to evaluate WM microstructure in a relatively large sample of treatment-naive PTSD patients without psychiatric comorbidity, compared with TENP controls, and to explore associations with symptom severity. As recent work finds that WM tract profiles have diagnostic potential (Chen et al., 2020; Dou et al., 2020), we also aimed to explore this. Following a previous study (Wakana et al., 2007), we selected 20 well-defined WM tracts and analyzed the diffusion measures along each. Based on previous evidence of disrupted WM organization, we hypothesized that: (i) compared with TENP, PTSD would exhibit alterations of fiber tracts previously shown to be abnormal in PTSD (e.g., uncinate fasciculus, cortico-spinal tract, superior and inferior longitudinal fasciculus, and arcuate fasciculus) which are implicated in behavioral deficits of PTSD (e.g., memory encoding and retrieval, stress response and emotion regulation) (Daniels et al., 2013; Hu et al., 2016; Koch et al., 2017; O'Doherty et al., 2018; Olson et al., 2017; Siehl et al., 2020); (ii) altered WM profiles would be associated with PTSD symptom severity; and (iii)

WM profiles could serve as neuroimaging biomarkers to distinguish PTSD patients from TENP controls. Finally, because being female increases the risk of developing PTSD (Tang et al., 2017) and there are possible differential effects of sex on WM alterations (Hsu et al., 2008), we (iv) analyzed sex-by-PTSD diagnosis interactions.

2 | MATERIALS AND METHODS

2.1 | Participants

Individuals who survived the 8.0 magnitude earthquake in Sichuan in May 2008 were recruited between January and August 2009 and screened with the PTSD checklist-Civilian Version (PCL) (Weathers et al., 1994). At follow-up visits 8–15 months after the earthquake, the diagnosis of PTSD was based on the Structured Clinical Interview for the DSM-IV Diagnosis (SCID) (First et al., 1994) and symptom severity was assessed using the Clinician-Administered PTSD Scale (CAPS) (Blake et al., 1995). Detailed inclusion and exclusion criteria are provided in Online Supporting Information. Briefly, survivors scoring ≥ 35 on PCL and ≥ 50 on CAPS were included as PTSD if a diagnosis of PTSD was determined by SCID; those who scored < 35 on PCL without diagnosis of PTSD by SCID were considered TENP controls. Finally included were 77 treatment-naive noncomorbid patients with PTSD and 76 demographically-matched TENP controls. This recruitment strategy ensured that participants with and without PTSD had similar earthquake experiences and demographic characteristics. This study was approved by the Sichuan University Research Ethics Committee. All participants provided written informed consent.

2.2 | Data acquisition

The magnetic resonance imaging (MRI) data were acquired on a three Tesla MRI system (GE EXCITE) with an 8-channel phased array head coil. DTI images were obtained with 15 noncollinear directions ($b = 1000$ s/mm^2) plus an acquisition without diffusion weighting ($b = 0$) with repetition time (TR) 12,000 ms, echo time (TE) 70.8 ms, slice thickness 3 mm, 50 slices, number of excitations 2, matrix size 128 × 128 and field of view (FOV) 24 × 24 cm^2. High-resolution T1-weighted anatomical images were acquired with a sagittal three-dimensional spoiled gradient recall sequence with TR 8.5 ms, TE 3.4 ms, inversion time 400 ms, slice thickness 1 mm, 156 axial slices, no inter-slice gap, matrix size 256 × 256, FOV 24 × 24 cm^2, and flip angle 12°. Foam cushions minimized head motion. An experienced neuroradiologist verified the quality of acquired images. We calculated head motion from the DTI data to exclude participants showing >2 mm displacement or translation in the x, y, or z directions, or >2° rotation around the x, y, or z axes; measured head motion did not differ between patients and controls (details in Table S1).

2.3 | Imaging processing and automatic tract identification

Routine DTI preprocessing, including brain extraction, head motion, and eddy current correction and diffusion tensor model fitting, was performed using FMRIB Software Library (FSL) (http://www.fmrib.ox. ac.uk/fsl). Automated Fiber Quantification software (Yeatman et al., 2012) was used to identify 20 WM tracts in each participant using the Johns Hopkins University WM template (http://neuro. debian.net/pkgs/fsl-jhu-dti-whitematter-atlas.html); as detailed previously (Yeatman et al., 2012) this involved whole-brain deterministic fiber tractography, waypoint region of interest-based tract segmentation, probability map–based tract refinement, outlier-rejection-based tract cleaning, and quantification of diffusion measures along each tract at 100 equally-spaced points. Tracts included the left and right anterior thalamic radiation, cingulum hippocampus, cingulum cingulate, corticospinal tract, superior longitudinal fasciculus, inferior longitudinal fasciculus, inferior fronto-occipital fasciculus, arcuate fasciculus, uncinate fasciculus, the forceps major of the splenium, and the forceps minor of the genu of the corpus callosum. Tracts were smoothed using a 10-point moving average filter.

2.4 | Statistical analysis

FA was compared between PTSD and TENP pointwise using the Randomize program in FSL as described previously (Sun et al., 2015). In brief, the tract profiles from each participant were arranged in a single matrix. These matrices were fed into permutation-based statistical analysis with 10,000 random permutations. Familywise error (FWE) correction for multiple comparisons was applied to determine the statistical significance thresholded at $p < .05$ (see Figure S1 for a flowchart). To probe the contributors to FA change, post hoc comparisons of axial diffusivity (AD), mean diffusivity (MD), and radial diffusivity (RD) were performed where FA differences were

significant. All diffusion measures were compared along the tract profiles. PTSD diagnosis-by-sex interaction was analyzed using two-way analysis of variance (ANOVA); if statistically significant interactions were observed, post hoc contrasts assessed the simple main effects. Partial correlation analysis was performed between the mean tract profiles (derived from the portion of the tracts which showed significant group differences) and CAPS and PCL scores to evaluate relationships between fiber tract microstructural organization and clinical symptom severity, with age, sex, years of education and time since trauma as covariates. Multiple comparison correction used the Bonferroni correction.

Exploratory support vector machine (SVM) analyses assessed how tract profiles could detect PTSD versus TENP at the individual level. By finding the hyperplane maximizing the margin between binary classes in the feature space, SVM can learn the classification strategy from the training set and utilize it to predict individual classification in a validation sample. Tract profiles of each participant were vectorized as features for model training. Five-fold stratified cross-validation was performed to split training and testing sets. The linear kernel was used to avoid overfitting. Classification performance was examined by average accuracy, sensitivity, and specificity based on testing sets across 5 folds. More details are provided in Online Supporting Information.

For a whole-brain WM analysis, Tract-Based Spatial Statistics (TBSS) was applied to compare the groups. Details and results are given in Online Supporting Information.

3 | RESULTS

3.1 | Group differences in demographics and clinical symptoms

Table 1 summarizes the demographic and clinical data of the 77 PTSD patients (mean ± SD age 42.3 ± 10.2 years, 52/25 women/men) and 76 TENP controls (age 43.7 ± 10.0 years, 56/20 women/men).

TABLE 1 Demographics and clinical characteristics of participants[a]

Variables	TENP (n = 76)	PTSD (n = 77)	p
Age (years)[b]	43.7 ± 10.0 (20–64)	42.3 ± 10.2 (19–65)	.38[c]
Sex (male/female)	20/56	25/52	.48[d]
Years of education[b]	6.6 ± 3.4 (0–12)	6.9 ± 3.2 (0–16)	.51[c]
Time since trauma (months)[b]	11.6 ± 2.3 (8–15)	11.2 ± 2.3 (8–15)	.35[c]
PTSD checklist	28.1 ± 6.9 (18–54)	47.3 ± 13.4 (21–80)	<.001[c]
CAPS	22.7 ± 11.5 (3–48)	63.1 ± 9.3 (51–95)	<.001[c]
Co-morbid diagnoses	0	0	

Abbreviations: CAPS, Clinician-administered PTSD scale; PTSD, posttraumatic stress disorder; SD, standard deviation; TENP, trauma-exposed non-PTSD controls.
[a]Data are presented as mean ± SD (minimum-maximum) unless noted.
[b]Age, years of education, and time since trauma at the time of MRI scanning.
[c]p value obtained using two-sample two-tailed t-test.
[d]p value calculated using two-tailed χ^2-test.

There were no significant between-group differences in age, sex, years of education, or time since trauma (*p* > .05).

3.2 | Pointwise comparison of tract profile alterations in TENP and PTSD

Figures S2–S5 show FA, AD, MD, and RD tract profiles for each participant group. Figure 1 and Table 2 show tract segments with significant between-group differences in tract profiles (FWE correction, *p* < .05). Compared to TENP, PTSD showed significantly *decreased FA* accompanied by *increased RD and MD* in the insular portion of the left uncinate fasciculus (nodes 27–44, Figure 1a), and *decreased FA* accompanied by *increased RD* in the posterior component of the right anterior thalamic radiation (nodes 84–90, Figure 1b). Figure 2 shows mean values for the tract segments showing significant between-group differences. AD tract profiles did not significantly differ between PTSD and TENP (*p* > .05).

3.3 | Interaction between groups and sex with respect to tract profiles

Two-way ANOVA revealed no significant diagnosis-by-sex interaction in FA (*p* = .53), MD (*p* = .84), or RD (*p* = .88) in the left uncinate fasciculus, or FA (*p* = .07) or RD (*p* = .30) in the right anterior thalamic radiation.

3.4 | Correlations between alterations in WM measures and symptom severity

As all subjects had experienced a major life trauma, with PTSD determined by the persistence and severity of psychological symptoms,

TABLE 2 Regions across the 20 fiber tracts where white matter measures differ significantly between PTSD patients and TENP controls

Diffusion measures/fiber tracts	TENP	PTSD
Left uncinate fasciculus (Nodes 27–44)		
Fractional anisotropy	0.424 ± 0.064	0.394 ± 0.051
Radial diffusivity	0.525 ± 0.082	0.560 ± 0.062
Mean diffusivity	0.696 ± 0.079	0.723 ± 0.064
Right anterior thalamic radiation (Nodes 84–90)		
Fractional anisotropy	0.454 ± 0.058	0.424 ± 0.048
Radial diffusivity	0.540 ± 0.056	0.567 ± 0.055

Note: Measurements presented as mean ± *SD*. Regions were considered abnormal if they exhibited significant between-group differences (*p* < .05) using permutation-based analysis (10,000 permutations) in FSL Randomize. Nodes are defined by dividing each tract into 100 equal segments between the beginning and termination waypoint regions of interest along the given tract.

Abbreviations: PTSD, posttraumatic stress disorder; TENP, trauma-exposed non-PTSD controls.
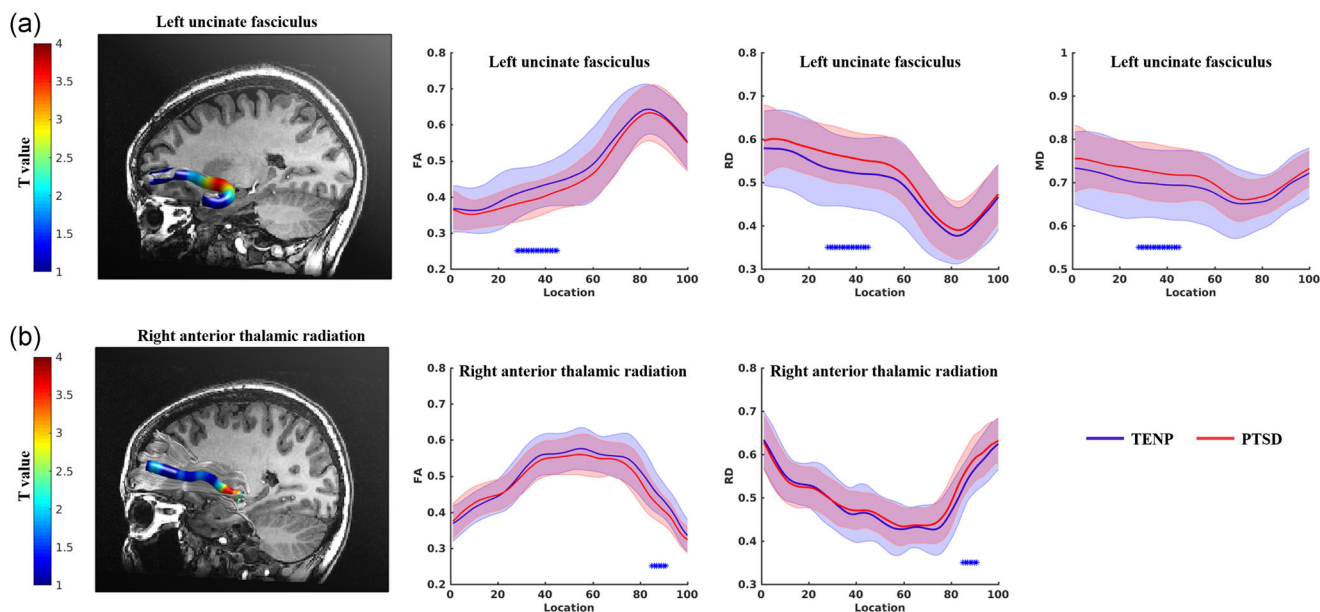

FIGURE 1 Point-wise comparison of white matter tract profiles between TENP controls and PTSD patients. The left panels show, for each tract as labeled, a three-dimensional rendering derived from automated fiber tract quantification software for a single representative participant. The right panels show the corresponding group tract profiles (blue for TENP, red for PTSD; solid lines showing means, shaded areas representing *SD*s). Each tract was divided into 100 equal segments (X axis) and tract profiles (Y axis) and scaled in the same way across tracts. The bars * under the fiber tracts indicate tract regions with pairwise white matter profiles of significant differences between TENP controls and PTSD patients. The x-axis represents the location between the beginning and termination waypoint regions of interest, following the Johns Hopkins University white matter template convention. FA, fractional anisotropy; MD, mean diffusivity; PTSD, posttraumatic stress disorder; RD, radial diffusivity; *SD*, standard deviation; TENP, trauma-exposed non-PTSD
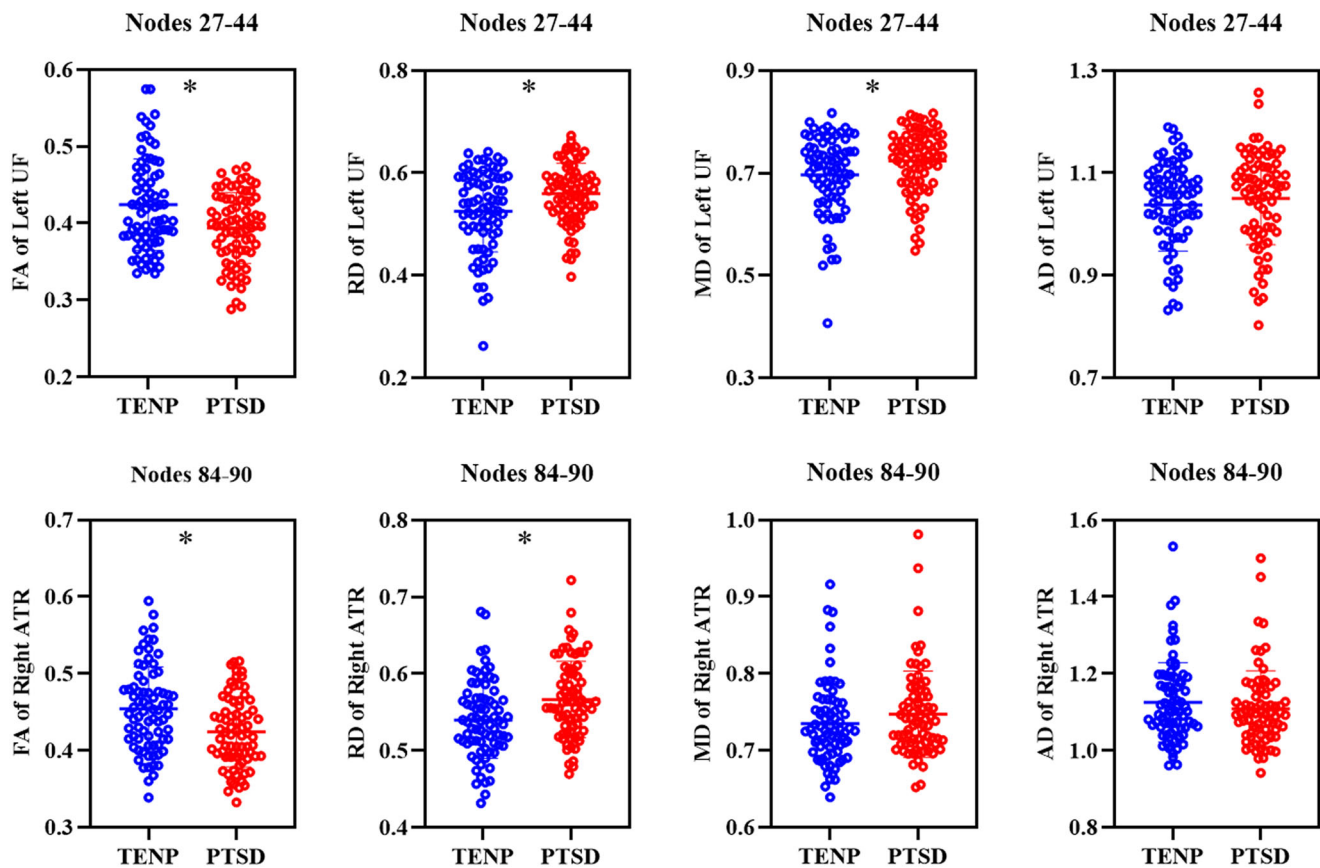
FIGURE 2 Mean values of the tract segments showing significant group differences between PTSD patients and TENP controls. *Indicates a statistical difference between groups, $p < .05$. AD, axial diffusivity; ATR, anterior thalamic radiation; FA, fractional anisotropy; MD, mean diffusivity; PTSD, posttraumatic stress disorder; RD, radial diffusivity; TENP, trauma-exposed non-PTSD; UF, uncinate fasciculus

the two subject groups were pooled to explore correlations between the mean tract profiles and PTSD symptom severity. As Figure 3 shows, there were moderate *negative correlations* between CAPS scores and mean FA over nodes 27–44 of the left uncinate fasciculus ($r = -0.267$, $p = .002$, Figure 3a), and mean FA for nodes 84–90 in the right anterior thalamic radiation ($r = -0.343$, $p < .001$, Figure 3b), as well as *a positive correlation* between CAPS scores and mean RD derived from nodes 27–44 in the left uncinate fasciculus ($r = .245$, $p = .004$, Figure 3c), and mean RD for nodes 84–90 in the right anterior thalamic radiation ($r = .247$, $p = .004$, Figure 3d), which survived Bonferroni correction ($p = .05/[5$ tract profile findings × 2 clinical symptoms] $= 0.005$). There were no significant correlations between CAPS score and mean MD for nodes 27–44 of left uncinate fasciculus.

There were no statistically significant relationships between PCL scores and tract profile alterations in PTSD or TENP ($p > .05$).

3.5 | Single-subject classification of TENP controls versus PTSD patients

Table S2 shows the results of the SVM based point-wise on the tract profiles. The mean balanced accuracy of classifications of TENP versus PTSD were all above chance; the AD profile showed the best

performance with mean balanced accuracy 73.8%, sensitivity 59.5%, and specificity 88.2%.

4 | DISCUSSION

We used automated fiber quantification to examine localized aberrations of WM microstructure in PTSD, and investigated their association with symptom severity, their diagnosis-by-sex interaction, and their potential as diagnostic biomarkers. The main findings were as follows: (i) PTSD compared with TENP showed disrupted WM profiles in the left uncinate fasciculus and right anterior thalamic radiation; (ii) these tract profile alterations were related to symptom severity, but (iii) showed no significant interactions between groups and sex; (iv) using tract profiles, the mean balanced accuracy of classifications of TENP versus PTSD were all above chance. This study adds to understanding of altered brain WM microstructure and its spatial localization in PTSD, and reveals potential biomarkers in diagnosis. We now discuss some specific findings.

Decreased FA and increased RD and MD in the insular portion of left uncinate fasciculus. The uncinate fasciculus is a ventral associative bundle connecting the anterior temporal and orbitofrontal regions involved in emotion regulation and memory formation (Von Der
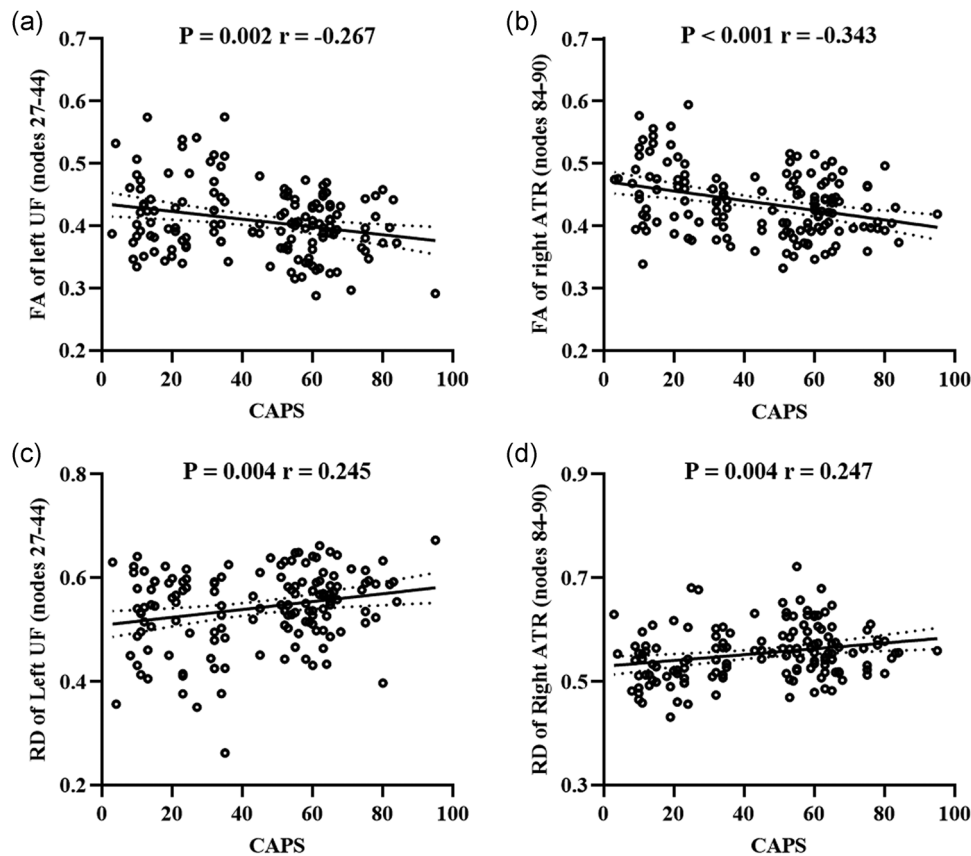
FIGURE 3 Relationships between the white matter tract profile alterations (mean values derived from the nodes significantly different between groups) and CAPS scores in the combined PTSD and TENP groups. ATR, anterior thalamic radiation; CAPS, clinician-administered PTSD scale; FA, fractional anisotropy; PTSD, posttraumatic stress disorder; RD, radial diffusivity; TENP, trauma-exposed non-PTSD; UF, uncinate fasciculus

Heide et al., 2013). Disrupted uncinate fasciculus microstructural organization has been related to impaired extinction learning, and the misinterpretation of social-emotional stimuli which may underpin avoidance behaviors in PTSD (Koch et al., 2017). Our study, and previous research (Costanzo et al., 2016; Harnett et al., 2020; O'Doherty et al., 2018), found disrupted organization in the uncinate fasciculus to be associated with symptom severity, suggesting a pathophysiological relevance. Consistent with this, a recent pilot trial reported a PTSD patient successfully treated with uncinate fasciculus deep brain stimulation (Hamani et al., 2020). A review of uncinate fasciculus development suggested that early life stress may be related to impaired WM microstructural organization owing to the vulnerability of limbic regions to stress hormones (Olson et al., 2015). Most studies have not emphasized specific regions of the uncinate fasciculus; automated fiber quantification allowed us to localize most of the changes to the insular portion.

Decreased FA and increased RD in the right anterior thalamic radiation. The anterior thalamic radiation connects the dorsomedial and anterior thalamic nuclei with the prefrontal cortex, passing through the anterior limb of the internal capsule (Coenen et al., 2012), which has a role in the expression of emotions (Spalletta et al., 2013). Decreased FA in the anterior thalamic radiation has been previously reported in PTSD (Hu et al., 2016). This is also compatible with our previous finding of

decreased functional connectivity in regions connected by fiber tracts (e.g. medial frontal cortex and thalamus); this may contribute to failed extinction memory and extinction retention and persistent excessive fear responses in PTSD (Yin et al., 2011). However, increased FA is reported in the right anterior thalamic radiation in PTSD relative to TENP (Yeh et al., 2020). A potential factor in such WM differences is the age of trauma (Siehl et al., 2018). All our patients experienced earthquake trauma in adulthood, while some studied by Yeh et al. experienced trauma below the age of 18 (Yeh et al., 2020). Note that although all participants experienced similar earthquake trauma, we cannot completely rule out the potentially confounding effects of childhood trauma exposure, as no specific standard scales (e.g., Childhood Trauma Questionnaire) were used to assess this. Our results need to be confirmed in future studies with a comprehensive evaluation of adulthood and childhood trauma.

Different WM microstructural organization markers. FA indicates the directionality of water diffusion, while MD measures the rate of water diffusion averaged in all directions. Loss of microstructural organization is typically accompanied by a decrease in FA and/or an increase in MD. AD and RD reflect water diffusion along the principal and perpendicular diffusion directions, respectively; AD is more sensitive to axonal damage, RD to myelin loss (Song et al., 2002). Low FA in left uncinate fasciculus and right anterior thalamic radiation was

accompanied by high RD (which seems to be related to demyelination [Harsan et al., 2007]) rather than low AD (which is taken to indicate axonal loss (Budde et al., 2009)). Stress-related demyelination is a feature of animal models of PTSD (Hemanth Kumar et al., 2014), so our findings may implicate myelin changes as underlying these subtle microstructural abnormalities in microstructural organization.

We did not find PTSD-related effects in the cortico-spinal tract, superior and inferior longitudinal fasciculus, and arcuate fasciculus, as some studies have (Choi et al., 2009; Hu et al., 2016; McCunn et al., 2021; Olson et al., 2017). These contradictory results may be explained by differences in the control group used (non-traumatized healthy controls vs. trauma-exposed normal controls), trauma type, duration of PTSD, comorbidities, and medication status (Ju et al., 2020), and technical differences in DTI acquisition and analysis.

We found no significant group-sex interaction with respect to tract profiles. Both presence and absence of diagnosis-by-sex interaction have been reported in PTSD (De Bellis & Kuchibhatla, 2006; Dennis et al., 2021; Luo et al., 2019), again, perhaps because of patient heterogeneity or technical factors. Few studies have directly investigated sex effects on brain structure in trauma-exposed cohorts (De Bellis & Keshavan, 2003; Klabunde et al., 2017). Sex differences have been reported in brain development in PTSD secondary to child abuse (De Bellis & Keshavan, 2003); however, changes in WM microstructure vary with age at traumatic experience (Siehl et al., 2018). Further studies are needed to define these effects in adults with trauma experience.

Significant correlations were found between diffusion measures and CAPS scores, but not with PCL. In terms of pathophysiology, this perhaps reflects the difference between a self-reported symptom inventory (PCL) and a structured clinical interview (CAPS). Clinically, their uses differ: structured interviews are recommended to establish a PTSD diagnosis, while self-report scales are better used to track changes in symptoms over time. In addition, PCL can evaluate early stress symptom severity before a PTSD diagnosis can be established after the required 1-month period, but questions have been raised regarding its specificity (McDonald et al., 2015).

This study revealed altered WM tract profiles which were associated with symptom severity, but whether tract profiles can serve as practical imaging biomarkers for individual patients is not yet clear. Promisingly, the mean balanced accuracy of classifications of TENP controls versus PTSD patients were all above chance. Machine learning is far from becoming a routine tool in clinical practice, but it may help to meet the urgent needs of clinical psychiatry by helping to develop imaging-based diagnostic biomarkers of early disease; this is a key aim of psychoradiology (Gong, 2020; Gong et al., 2021; Huang et al., 2019; Lan et al., 2021; Li et al., 2021; Lui et al., 2016; Pan et al., 2021; Suo et al., 2021), the emerging radiological subspecialty guiding diagnosis and treatment decisions in neuropsychiatric patients. Future studies should explore whether our findings are specific to PTSD, rather than trans-diagnostic features of psychiatric disorders.

Our study has limitations. First, it was cross-sectional: how WM microstructure changes after major life stress evolve and predict future PTSD conversion must be addressed in longitudinal studies. Second, the correlations between altered tract profiles and CAPS scores were relatively modest, so this analysis should be considered exploratory. Third, the purpose of our research was to determine WM microstructure characteristics that distinguish stressed individuals who do and do not develop PTSD. Without a parallel group of non-traumatized individuals, we cannot identify differences between these two groups and healthy controls, to identify how major life stress itself impacts WM microstructural organization. Fourth, our sample was homogeneous in that all subjects were exposed to the earthquake; however, one should be cautious in generalizing our findings to PTSD caused by other types of trauma. Fifth, the accuracy of the SVM classification methods was not particularly high, and better performance may be achieved via other advanced techniques such as deep learning, although these typically involve higher levels of abstraction and complexity and the computation of a large number of parameters that requires a bigger sample (Vieira et al., 2017). Sixth, studying participants free from psychiatric comorbidity improved sample homogeneity, but leaves open whether our findings generalize to PTSD with psychiatric comorbidities. Additionally, some confounding factors, for example, childhood trauma (Morey et al., 2016; Sun et al., 2019), cannot be excluded in our analysis. Finally, cognition deficits are a new focus in PTSD research; we did not include any cognitive evaluation. Future studies should address these issues.

5 | CONCLUSION

Using a tract-profile quantification approach and SVM analyses, this study detected altered diffusion metrics of fiber tracts in PTSD patients, providing evidence of abnormal WM microstructure in the left uncinate fasciculus and right anterior thalamic radiation, which were associated with symptom severity, but with no significant interaction between groups and sex. Our findings provide a more detailed understanding of WM changes in PTSD with potential as diagnostic biomarkers.

CONFLICT OF INTERESTS

The authors declare that there are no conflict of interests.

DATA AVAILABILITY STATEMENT

The data that support the findings of this study are available from the corresponding author upon reasonable request.

ORCID

Qiyong Gong http://orcid.org/0000-0002-5912-4871

REFERENCES

American Psychiatric Association. (2013). *Diagnostic and statistical manual of mental disorders DSM-5* (5th ed.). American Psychiatric Publishing.

Blake, D. D., Weathers, F. W., Nagy, L. M., Kaloupek, D. G., Gusman, F. D., Charney, D. S., & Keane, T. M. (1995). The development of a Clinician-Administered PTSD Scale. *Journal of Traumatic Stress*, 8(1), 75–90. https://doi.org/10.1007/BF02105408

Budde, M. D., Xie, M., Cross, A. H., & Song, S.-K. (2009). Axial diffusivity is the primary correlate of axonal injury in the experimental autoimmune encephalomyelitis spinal cord: A quantitative pixelwise analysis. *Journal of Neuroscience*, 29(9), 2805–2813. https://doi.org/10.1523/JNEUROSCI.4605-08.2009

Chen, H., Sheng, X., Qin, R., Luo, C., Li, M., Liu, R., Zhang, B., Xu, Y., Zhao, H., & Bai, F. (2020). Aberrant white matter microstructure as a potential diagnostic marker in Alzheimer's disease by automated fiber quantification. *Frontiers in Neuroscience*, 14, 570123. https://doi.org/10.3389/fnins.2020.570123

Choi, J., Jeong, B., Rohan, M. L., Polcari, A. M., & Teicher, M. H. (2009). Preliminary evidence for white matter tract abnormalities in young adults exposed to parental verbal abuse. *Biological Psychiatry*, 65(3), 227–234. https://doi.org/10.1016/j.biopsych.2008.06.022

Coenen, V. A., Panksepp, J., Hurwitz, T. A., Urbach, H., & Madler, B. (2012). Human medial forebrain bundle (MFB) and anterior thalamic radiation (ATR): Imaging of two major subcortical pathways and the dynamic balance of opposite affects in understanding depression. *Journal of Neuropsychiatry and Clinical Neurosciences*, 24(2), 223–236. https://doi.org/10.1176/appi.neuropsych.11080180

Costanzo, M. E., Jovanovic, T., Pham, D., Leaman, S., Highland, K. B., Norrholm, S. D., & Roy, M. J. (2016). White matter microstructure of the uncinate fasciculus is associated with subthreshold posttraumatic stress disorder symptoms and fear potentiated startle during early extinction in recently deployed Service Members. *Neuroscience Letters*, 618, 66–71. https://doi.org/10.1016/j.neulet.2016.02.041

Daniels, J. K., Lamke, J. P., Gaebler, M., Walter, H., & Scheel, M. (2013). White matter integrity and its relationship to PTSD and childhood trauma: A systematic review and meta-analysis. *Depression and Anxiety*, 30(3), 207–216. https://doi.org/10.1002/da.22044

De Bellis, M. D., & Keshavan, M. S. (2003). Sex differences in brain maturation in maltreatment-related pediatric posttraumatic stress disorder. *Neuroscience and Biobehavioral Reviews*, 27(1-2), 103–117. https://doi.org/10.1016/s0149-7634(03)00013-7

De Bellis, M. D., & Kuchibhatla, M. (2006). Cerebellar volumes in pediatric maltreatment-related posttraumatic stress disorder. *Biological Psychiatry*, 60(7), 697–703. https://doi.org/10.1016/j.biopsych.2006.04.035

Dennis, E. L., Disner, S. G., Fani, N., Salminen, L. E., Logue, M., Clarke, E. K., Haswell, C. C., Averill, C. L., Baugh, L. A., Bomyea, J., Bruce, S. E., Cha, J., Choi, K., Davenport, N. D., Densmore, M., du Plessis, S., Forster, G. L., Frijling, J. L., Gonenc, A., ... Morey, R. A. (2021). Altered white matter microstructural organization in posttraumatic stress disorder across 3047 adults: results from the PGC-ENIGMA PTSD consortium. *Molecular Psychiatry*, 26(8), 4315–4330. https://doi.org/10.1038/s41380-019-0631-x

Dou, X., Yao, H., Feng, F., Wang, P., Zhou, B., Jin, D., Yang, Z., Li, J., Zhao, C., Wang, L., An, N., Liu, B., Zhang, X., & Liu, Y. (2020). Characterizing white matter connectivity in Alzheimer's disease and mild cognitive impairment: An automated fiber quantification analysis with two independent datasets. *Cortex*, 129, 390–405. https://doi.org/10.1016/j.cortex.2020.03.032

First, M. B., Spitzer, R. L., Gibbon, M., & Williams, J. B. (1994). Structured clinical interview for Axis I DSM-IV disorders. Biometrics Research.

Gong, Q. (2020). Psychoradiology. *Neuroimaging Clinics of North America*, 30, 1–123. Elsevier Inc.

Gong, Q., Kendrick, K. M., & Lu, L. (2021). Psychoradiology: A new era for neuropsychiatric imaging. *Psychoradiology*, 1(1), 1–2. https://doi.org/10.1093/psyrad/kkaa001

Hamani, C., Davidson, B., Levitt, A., Meng, Y., Corchs, F., Abrahao, A., Rabin, J. S., Giacobbe, P., & Lipsman, N. (2020). Patient with posttraumatic stress disorder successfully treated with deep brain stimulation of the medial prefrontal cortex and uncinate fasciculus. *Biological Psychiatry*, 88(11), e57–e59. https://doi.org/10.1016/j.biopsych.2020.05.018

Harnett, N. G., Ference, E. W., 3rd, Knight, A. J., & Knight, D. C. (2020). White matter microstructure varies with post-traumatic stress severity following medical trauma. *Brain imaging and behavior*, 14(4), 1012–1024. https://doi.org/10.1007/s11682-018-9995-9

Harsan, L. A., Poulet, P., Guignard, B., Parizel, N., Skoff, R. P., & Ghandour, M. S. (2007). Astrocytic hypertrophy in dysmyelination influences the diffusion anisotropy of white matter. *Journal of Neuroscience Research*, 85(5), 935–944. https://doi.org/10.1002/jnr.21201

Hemanth Kumar, B. S., Mishra, S. K., Trivedi, R., Singh, S., Rana, P., & Khushu, S. (2014). Demyelinating evidences in CMS rat model of depression: A DTI study at 7 T. *Neuroscience*, 275, 12–21. https://doi.org/10.1016/j.neuroscience.2014.05.037

Hsu, J. L., Leemans, A., Bai, C. H., Lee, C. H., Tsai, Y. F., Chiu, H. C., & Chen, W. H. (2008). Gender differences and age-related white matter changes of the human brain: A diffusion tensor imaging study. *NeuroImage*, 39(2), 566–577. https://doi.org/10.1016/j.neuroimage.2007.09.017

Hu, H., Zhou, Y., Wang, Q., Su, S., Qiu, Y., Ge, J., Wang, Z., & Xiao, Z. (2016). Association of abnormal white matter integrity in the acute phase of motor vehicle accidents with post-traumatic stress disorder. *Journal of Affective Disorders*, 190, 714–722. https://doi.org/10.1016/j.jad.2015.09.044

Huang, X., Gong, Q., Sweeney, J. A., Biswal, B. B. (2019). Progress in psychoradiology, the clinical application of psychiatric neuroimaging. *The British Journal of Radiology*, 92, (1101), 20181000. http://dx.doi.org/10.1259/bjr.20181000

Ju, Y., Ou, W., Su, J., Averill, C. L., Liu, J., Wang, M., Wang, Z., Zhang, Y., Liu, B., Li, L., & Abdallah, C. G. (2020). White matter microstructural alterations in posttraumatic stress disorder: An ROI and whole-brain based meta-analysis. *Journal of Affective Disorders*, 266, 655–670. https://doi.org/10.1016/j.jad.2020.01.047

Kessler, R. C. (2000). Posttraumatic stress disorder: The burden to the individual and to society. *Journal of Clinical Psychiatry*, 61(Suppl 5), 4–12.

Klabunde, M., Weems, C. F., Raman, M., & Carrion, V. G. (2017). The moderating effects of sex on insula subdivision structure in youth with posttraumatic stress symptoms. *Depression and Anxiety*, 34(1), 51–58. https://doi.org/10.1002/da.22577

Koch, S. B. J., van Zuiden, M., Nawijn, L., Frijling, J. L., Veltman, D. J., & Olff, M. (2017). Decreased uncinate fasciculus tract integrity in male and female patients with PTSD: A diffusion tensor imaging study. *Journal of Psychiatry and Neuroscience*, 42(5), 331–342. https://doi.org/10.1503/jpn.160129

Lan, H., Suo, X., Li, W., Li, N., Li, J., Peng, J., Lei, D., Sweeney, J. A., Kemp, G. J., Peng, R., & Gong, Q. (2021). Abnormalities of intrinsic brain activity in essential tremor: A meta-analysis of resting-state functional imaging. *Human Brain Mapping*, 42(10), 3156–3167. https://doi.org/10.1002/hbm.25425

Li, F., Sun, H., Biswal, B. B., Sweeney, J. A., & Gong, Q. (2021). Artificial intelligence applications in psychoradiology. *Psychoradiology*, 1(2), 94–107. https://doi.org/10.1093/psyrad/kkab009

Lui, S., Zhou, X., Sweeney, J. A., & Gong, Q. (2016). Psychoradiology: The Frontier of Neuroimaging in Psychiatry. *Radiology*, 281(2), 357–372. https://doi.org/10.1148/radiol.2016152149

Luo, Y., Qi, R., Zhang, L., Qing, Z., Weng, Y., Wang, W., Zhang, X., Shan, H., Li, L., Cao, Z., & Lu, G. (2019). Functional brain network topology in parents who lost their only child in China: Post-traumatic stress

disorder and sex effects. *Journal of Affective Disorders*, 257, 632–639. https://doi.org/10.1016/j.jad.2019.07.004

McCunn, P., Richardson, J. D., Jetly, R., & Dunkley, B. (2021). Diffusion tensor imaging reveals white matter differences in military personnel exposed to trauma with and without post-traumatic stress disorder. *Psychiatry Research*, 298, 113797. https://doi.org/10.1016/j.psychres.2021.113797

McDonald, S. D., Brown, W. L., Benesek, J. P., & Calhoun, P. S. (2015). A systematic review of the PTSD checklist's diagnostic accuracy studies using QUADAS. *Psychol Trauma*, 7(5), 413–421. https://doi.org/10.1037/tra0000001

Meng, L., Shan, T., Li, K., & Gong, Q. (2020). Long-term tract-specific white matter microstructural changes after acute stress. *Brain imaging and behavior*, 15(4), 1868–1875. https://doi.org/10.1007/s11682-020-00380-w

Morey, R. A., Haswell, C. C., Hooper, S. R., & De Bellis, M. D. (2016). Amygdala, hippocampus, and ventral medial prefrontal cortex volumes differ in maltreated youth with and without chronic posttraumatic stress disorder. *Neuropsychopharmacology*, 41(3), 791–801. https://doi.org/10.1038/npp.2015.205

O'Doherty, D. C. M., Ryder, W., Paquola, C., Tickell, A., Chan, C., Hermens, D. F., Bennett, M. R., & Lagopoulos, J. (2018). White matter integrity alterations in post-traumatic stress disorder. *Human Brain Mapping*, 39(3), 1327–1338. https://doi.org/10.1002/hbm.23920

Olson, E. A., Cui, J. L., Fukunaga, R., Nickerson, L. D., Rauch, S. L., & Rosso, I. M. (2017). Disruption of white matter structural integrity and connectivity in posttraumatic stress disorder: A TBSS and tractography study. *Depression and Anxiety*, 34(5), 437–445. https://doi.org/10.1002/da.22615

Olson, I. R., Von Der Heide, R. J., Alm, K. H., & Vyas, G. (2015). Development of the uncinate fasciculus: Implications for theory and developmental disorders. *Dev Cogn Neurosci*, 14, 50–61. https://doi.org/10.1016/j.dcn.2015.06.003

Pan, N., Wang, S., Zhao, Y., Lai, H., Qin, K., Li, J., Biswal, B. B., Sweeney, J. A., & Gong, Q. (2021). Brain gray matter structures associated with trait impulsivity: A systematic review and voxel-based meta-analysis. *Human Brain Mapping*, 42(7), 2214–2235. https://doi.org/10.1002/hbm.25361

Ross, M. C., & Cisler, J. M. (2020). Altered large-scale functional brain organization in posttraumatic stress disorder: A comprehensive review of univariate and network-level neurocircuitry models of PTSD. *NeuroImage: Clinical*, 27, 102319. https://doi.org/10.1016/j.nicl.2020.102319

Siehl, S., King, J. A., Burgess, N., Flor, H., & Nees, F. (2018). Structural white matter changes in adults and children with posttraumatic stress disorder: A systematic review and meta-analysis. *NeuroImage: Clinical*, 19, 581–598. https://doi.org/10.1016/j.nicl.2018.05.013

Siehl, S., Wicking, M., Pohlack, S., Winkelmann, T., Zidda, F., Steiger-White, F., King, J., Burgess, N., Flor, H., & Nees, F. (2020). Structural white and gray matter differences in a large sample of patients with posttraumatic stress disorder and a healthy and trauma-exposed control group: Diffusion tensor imaging and region-based morphometry. *NeuroImage: Clinical*, 28, 102424. https://doi.org/10.1016/J.Nicl.2020.102424

Song, S.-K., Sun, S.-W., Ramsbottom, M. J., Chang, C., Russell, J., & Cross, A. H. (2002). Dysmyelination revealed through MRI as increased radial (but unchanged axial) diffusion of water. *NeuroImage*, 17(3), 1429–1436. https://doi.org/10.1006/nimg.2002.1267

Spalletta, G., Fagioli, S., Caltagirone, C., & Piras, F. (2013). Brain microstructure of subclinical apathy phenomenology in healthy individuals. *Human Brain Mapping*, 34(12), 3193–3203. https://doi.org/10.1002/hbm.22137

Sun, D. L., Haswell, C. C., Morey, R. A., & de Bellis, M. D. (2019). Brain structural covariance network centrality in maltreated youth with PTSD and in maltreated youth resilient to PTSD. *Development and Psychopathology*, 31(2), 557–571. https://doi.org/10.1017/S0954579418000093

Sun, H., Lui, S., Yao, L., Deng, W., Xiao, Y., Zhang, W., Huang, X., Hu, J., Bi, F., Li, T., Sweeney, J. A., & Gong, Q. (2015). Two patterns of white matter abnormalities in medication-naive patients with first-episode schizophrenia revealed by diffusion tensor imaging and cluster analysis. *JAMA Psychiatry*, 72(7), 678–686. https://doi.org/10.1001/jamapsychiatry.2015.0505

Suo, X., Lei, D., Li, W., Li, L., Dai, J., Wang, S., Li, N., Cheng, L., Peng, R., Kemp, G. J., & Gong, Q.(2021). Altered white matter microarchitecture in Parkinson's disease: a voxel-based meta-analysis of diffusion tensor imaging studies. *Frontiers of Medicine*, 15, 125–138. https://doi.org/10.1007/s11684-019-0725-5

Tang, B., Deng, Q., Glik, D., Dong, J., & Zhang, L. (2017). A meta-analysis of risk factors for post-traumatic stress disorder (PTSD) in adults and children after earthquakes. *International Journal of Environmental Research and Public Health*, 14(12):1537. https://doi.org/10.3390/ijerph14121537

Vieira, S., Pinaya, W. H. L., & Mechelli, A. (2017). Using deep learning to investigate the neuroimaging correlates of psychiatric and neurological disorders: Methods and applications. *Neuroscience and Biobehavioral Reviews*, 74(Pt A), 58–75. https://doi.org/10.1016/j.neubiorev.2017.01.002

Von Der Heide, R. J., Skipper, L. M., Klobusicky, E., & Olson, I. R. (2013). Dissecting the uncinate fasciculus: Disorders, controversies and a hypothesis. *Brain*, 136(Pt 6), 1692–1707. https://doi.org/10.1093/brain/awt094

Wakana, S., Caprihan, A., Panzenboeck, M. M., Fallon, J. H., Perry, M., Gollub, R. L., Hua, K. G., Zhang, J. Y., Jiang, H. Y., Dubey, P., Blitz, A., van Zijl, P., & Mori, S. (2007). Reproducibility of quantitative tractography methods applied to cerebral white matter. *NeuroImage*, 36(3), 630–644. https://doi.org/10.1016/j.neuroimage.2007.02.049

Weathers, F. W., Litz, B. T., Herman, D., Huska, J., & Keane, T. (1994). The PTSD checklist-civilian version (PCL-C). National Center for PTSD.

Yeatman, J. D., Dougherty, R. F., Myall, N. J., Wandell, B. A., & Feldman, H. M. (2012). Tract profiles of white matter properties: automating fiber-tract quantification. *PLoS One*, 7, e49790 https://doi.org/10.1371/journal.pone.0049790

Yeh, C. L., Levar, N., Broos, H. C., Dechert, A., Potter, K., Evins, A. E., & Gilman, J. M. (2020). White matter integrity differences associated with post-traumatic stress disorder are not normalized by concurrent marijuana use. *Psychiatry Research, Neuroimaging*, 295, 111017. https://doi.org/10.1016/j.pscychresns.2019.111017

Yin, Y., Jin, C., Hu, X., Duan, L., Li, Z., Song, M., Chen, H., Feng, B., Jiang, T., Jin, H., Wong, C., Gong, Q., & Li, L. (2011). Altered resting-state functional connectivity of thalamus in earthquake-induced posttraumatic stress disorder: a functional magnetic resonance imaging study. *Brain Research*, 1411, 98–107. https://doi.org/10.1016/j.brainres.2011.07.016

SUPPORTING INFORMATION

Additional supporting information may be found in the online version of the article at the publisher's website.